The Materials Research Society (MRS)
XXII INTERNATIONAL MATERIALS RESEARCH CONGRESS 2013
NACE International Congress-Mexican Section

MICROSTRUCTURE AND MECHANICAL BEHAVIOR OF 2024 ALUMINUM ALLOY REINFORCED WITH ALUMINA NANOPARTICLES BY MECHANICAL MILLING

Carlos Alberto López Medina. Centro de Investigación en Materiales Avanzados (CIMAV), Miguel de Cervantes 120, Complejo Industrial Chihuahua, México; C.P. 31109. Tel: +52 6144391102. Ingeniería Metal-Mecánica, Universidad Tecnológica de Torreón, Carretera Torreón-Matamoros KM.10 Ejido el Águila, C.P. 27410, Torreón México.clopez@utt.edu.mx.

Miguel Ángel Neri Flores. Centro de Investigación en Materiales Avanzados (CIMAV), Miguel de Cervantes 120, Complejo Industrial Chihuahua, México; C.P. 31109. Tel: +52 6144391102. miguel.neri@cimav.edu.mx

José Luis Hernández Rivera. Centro de Investigación en Materiales Avanzados (CIMAV), Miguel de Cervantes 120, Complejo Industrial Chihuahua, México; C.P. 31109. Tel: +52 6144391102. jose.hernadez@cimav.edu.mx

Roberto Martínez Sánchez. Centro de Investigación en Materiales Avanzados (CIMAV), Miguel de Cervantes 120, Complejo Industrial Chihuahua, México; C.P. 31109. Tel: +52 6144391102. roberto.martinez@cimav.edu.mx

Abstract

2024 Aluminum alloy reinforced with alumina nanoparticles (15nm) was produced by mechanical milling (MM) to obtain a metal matrix composite (MMC). The selected alumina content was 0.0, 1.0, 2.0, 3.0, 4.0 and 5.0 wt.%. Consolidated bulk material was obtained by pressing the milled powder under an uniaxial load, after that, sintering and hot extruding were applied using indirect extrusion with a ratio of 1:16 to obtain the final material. The microstructural characterization was done by transmission electron microscopy (TEM), scanning transmission electron microscopy (STEM), scanning electron microscopy (SEM), chemical analysis by characteristic X-ray energy dispersion spectroscopy (EDS) and X-ray diffraction (XRD). The best results were obtained at 2.0 wt.% of alumina that is the critical value of ceramic nanoparticle reinforcement in this material. At this point the yield and tensile strength were 220.9 and 443.6 MPa respectively. With 3.0 wt.% or bigger values in alumina reinforcement particles, the green bulked material has lower densification of the aluminum powder, the agglomeration of

nanoparticles takes place, and reduces the effectiveness with the strength in the MMC. The most important strengthening mechanisms were: the hardening by dispersion of the second phase, the subsequent effect over the dislocations line movement, grain refinement, thermal mismatch between aluminum alloy and alumina nanoparticles, the Orowan looping, and intermetallics crystallization.

1. Introduction

It is well known that aluminum alloys and composites can be strengthened by dispersing hard particles, such as carbides, oxides and nitrides into the aluminum matrix using different techniques in the solid state [1-3]. The mechanical milling method has been considered a powerful and practical process to obtain several advanced materials with unique properties. This type of composite production process involves the mixing of reinforcement particles with the metallic powder, followed by consolidation and sintering processes. Different kind of ceramic particles such as: SiC, Ni_3Al, B_4C, Si_3Ni, and CNTs have been used as reinforcement phase. [2,4,5]

The decrease size of the reinforcement from micrometric to nanometric scale, gives superior values in the mechanical properties of the composite, but on the other hand, the tendency of particle clustering and agglomeration in materials composites have been addressed by Jia et al.[6]

According to Khakbiz and Akhlaghi[7], it is important the fact that homogeneous distribution of the reinforcement particles is essential to achieve the improved properties, in that way mechanical alloying via ball milling has been employed successfully to improve particle distribution throughout the matrix.

Naser et al. [8] have shown that this method is a novel approach for dispersion strengthening of metals by nano-oxides where the internal oxidation technique is not applicable. Tang et al.[9] reported the homogenous distribution of SiC nanoparticles into Al-5083 matrix by the milling process; Ferkel and Mordike [10] strengthened magnesium by SiC nanoparticles via mechanical milling. So, it has been determined that nanomaterials can be distributed into the metal matrix composites sufficiently after a relative short period of milling time.

The main focus of this research is the mechanical and microstructural characterization on the Al-2024 composite produced by dispersion of alumina nanoparticles, focus on

nanoparticles dispersion and the effect in mechanical properties. The best result in mechanical properties as a function of weight percentage of alumina is presented. Morphology, dispersion and adhesion of the Al_2O_3 nanoparticles are presented and briefly discussed from a microstructural point of view. Several strengthening mechanisms are analyzed in the aluminum matrix composite working at the same time.

2. Experimental Procedure

2024 Aluminum alloy and γ-Al2O3 nanoparticles were used as raw materials. The chemical composition of 2024 Aluminum alloy is shown in Table 1.

The nanometric particles of γ-Al2O3 (mkNano, MKN Al2O3-015) have an average size of 15 nm. The selected alumina contents are 0.0, 1.0, 2.0, 3.0, 4.0 and 5.0 wt.%. Each mixture was mechanically milled in a high energy Simoloyer mill, for 10 h in an argon atmosphere. The mixture weight was set to 80 g. 0.5 ml of pure methanol was used as a process control agent (PCA), in order to minimize cold welding between powder particles and inhibit the agglomeration in the material. The milling weight ratio of balls and powder was set at 20:1.

Table 1. Chemical composition of 2024 Al alloy (wt %).

Elements	Nominal (wt.%)	Experimental (wt.%)
Al	Balance	Balance
Cu	3.80 - 4.90	4.153
Mg	1.20 - 1.80	0.915
Mn	0.30 – 0.90	0.710
Fe	<0.50	0.191
Si	<0.50	0.131
Zn	<0.25	0.130
Cr	<0.10	0.033
Ti	<0.15	0.045

Consolidated bulk material was obtained by pressing the milled powder at ~850 MPa in an uniaxial load for 5 minutes. Pressed samples were next sintered under vacuum (~ 1 torr) for 1 h at 523K after that, 2h at 773 K with a heating rate of 50 K/min. Sintered

material was held 30 minutes at 823K and hot extruded into a rod of 10 mm of diameter by using indirect extrusion with an extrusion ratio of 1:16.

The mechanical tests, including tensile and microhardness analysis, were carried out at room temperature along of the extrusion direction. Instron universal testing machine was set at an overhead displacement of 0.016mm/s. The bone shape samples were used according to ASTM B557M standards. The yield strength was measured at ε=0.2% and the maximum strength at the maximum value of the σ-ε plot. The microhardness measurements were done using Future-Tech Corp model FM-7 with load of 50g. with 15s. of dwell time, the average values of at least five points of random selected regions on each sample are reported. The structural characterization was done by transmission electron microscopy (TEM) JEOL JEM 2200FS operated at 200 kV, scanning electron microscopy (SEM) JEOL JSM-7401F, operated at 20 kV. During SEM analyses, both SEM and STEM mode were used. Semiquantitative chemical analyses were done by energy dispersive spectroscopy (EDS) using an Oxford Inca X-Ray energy dispersive spectrometer coupled to a SEM system. X-ray diffraction was done in a Panalytical X'Pert Pro diffractometer with Cu$K\alpha$ radiation (λ=0.15406 nm) operated at 40 kV and 35 mA in the range of 30-110°, 5s for collecting time and 0.05° of step size were used. Thin foils samples for TEM were prepared from extruded bars by electropolishing using a mixture of 25 vol. % of nitric acid in methanol at 223K and 20 VCD.

3. Results and discussion

3.1 Mechanical Behavior

Fig. 1 shows the tensile test results of all samples in extruded condition. The aluminum composites exhibit an increment about 10% in yield strength and tensile strength, compared with original aluminum alloy. The strength of the composites increases with the weight percentage of alumina nanoparticles. But once the 2.0 wt. % of the reinforcement particles was exceeded, the composite's strength showed an important decrement. In the same way, Fig. 1 shows a decrement in elongation property. The elongation changes from 15.3 % at 0.0 wt.% of alumina, to 7.3% with 5.0 wt.% of alumina reinforcement phase, due to strengthening mechanism; specially related with the nanoparticles phases. Some investigations [10-13] have indicated that the strengths of composites increased with mass fraction of particles. But once the critical percent of nanoparticles in the composites was exceeded, the strength of aluminum composite was diminished. It is well known that the mechanical properties depend strongly on the amount, type size and distribution of

the reinforcement particles presented in the metal matrix composite (MMC), these factors could be the explanation to the decrease about its mechanical behavior.

According to Table 2, the yield strength increased from 184.2 MPa to 200.9 MPa which correspond to an increment of about 10%; and tensile strength from 388.2 MPa to 443.6 MPa corresponding to an increment of 15%, at 2 wt.% of alumina, that is considered as the critical value of the reinforcement phase. Furthermore, comparing the annealing condition (Al-2024-O) with MMC at 2.0 wt.% of alumina, the improvements are 165% in yield strength, and 138.5% in the tensile strength respectively. In the same way, the variations of Al-2024-T6 condition with the MMC at the same percentage of nanoparticles are: 36.22% of diminution in yield strength and 6.9% increase in tensile strength. Above the critical value of reinforcement phase, agglomeration takes place [2-3, 11], and it is more evident when the reinforced phase is in the nanometric range.

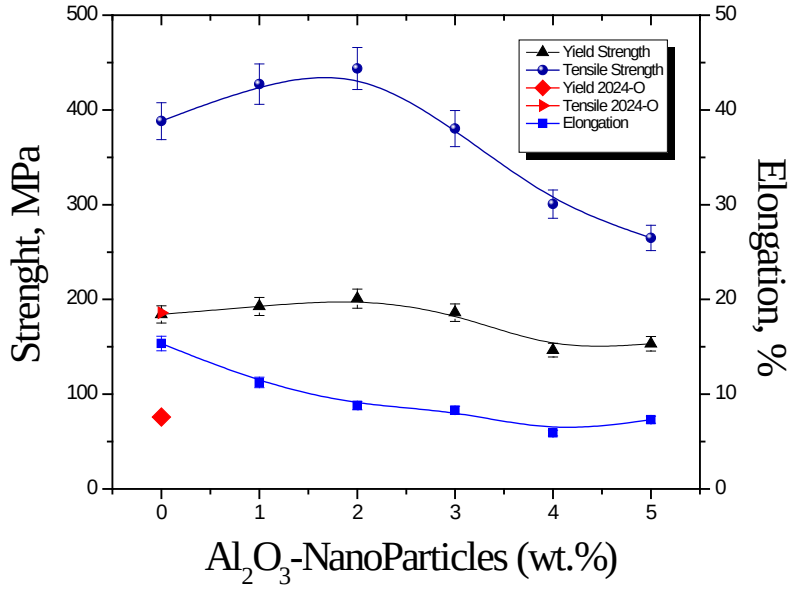

Fig. 1 Tensile Properties of the aluminum composite, as a function of wt% of alumina, (◆) and (►) Mechanical Properties [12] for Al-2024 in annealing condition.

The micro-hardness results of the composites are shown in Fig. 2 at different concentrations of nanoparticles. This graph shows the maximum value (185 HV) in the composite with 3.0 wt. % of Al_2O_3. The hardness values increase as the alumina content increases, but in 4 and 5 wt.% Al_2O_3 these amounts decrease (Table 2), because of the agglomeration of the nanoparticles. The maximum value was compared with the aluminum alloy in annealed condition (Al-2024-O) and Al-2024-T6 temper; the average

increments were 253% and 30.3% correspondingly. The increments are associated to combined effects like: homogeneous distribution of the nanoparticles into the aluminum matrix, the refinement of the crystal size, the crystallization of second phases in alloy, and density increase of dislocation due to the thermal mismatch of aluminum and alumina reinforcement, and also the dislocation blocking due to the presence of nanoparticles and second phases finely dispersed into the aluminum.

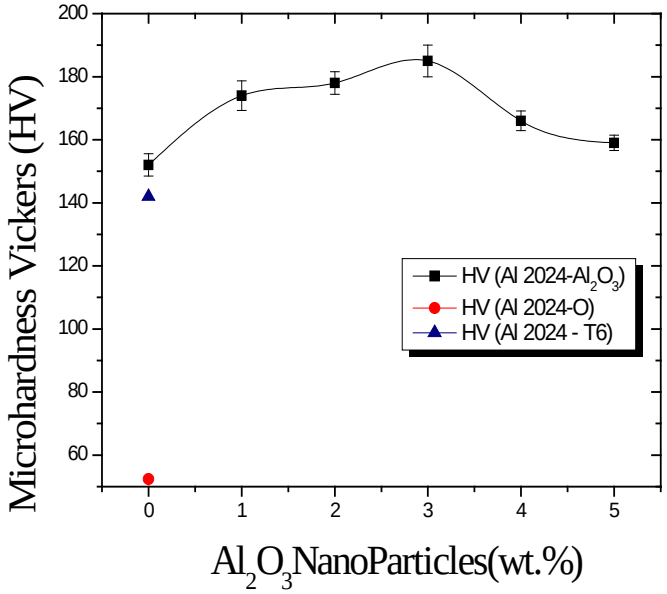

Fig. 2 Micro-hardness Vickers in extruded samples as a function of wt.% alumina. Hardness for Al-2024 in annealing condition (●) and T6 temper (▲) [12].

*Table 2. Mechanical properties of 2024-Al at different wt. % of alumina nanoparticles. ** Mechanical Properties of Al-2024-O and Al-2024-T6 Temper [12]*

Material	wt.% Alumina	Yield Strength (MPa)	Tensile Strength (MPa)	Micro Hardness Vickers (HV)
Al-2024-O	**	75.8	186	52.4
Al-2024-T6	**	315.0	415.0	142
M0-2024	0.0	184.2	388.2	152
M1-2024	1.0	192.6	427.3	174
M2-2024	2.0	200.9	443.6	178
M3-2024	3.0	186.1	380.4	185
M4-2024	4.0	146.5	300.6	156
M5-2024	5.0	153.2	264.9	159

3.2 X-ray Diffraction Pattern

The x ray diffraction patterns of the MMCs with different percentage of alumina nanoparticles are shown in Fig. 3. The principal reflections in the different samples are the aluminum matrix and some precipitates like: Al_2CuMg (S'), Al_2Cu (θ') and $Al_{20}Cu_2Mn_3$(T). These precipitates are observed, due to the sintering and hot extrusion processes. It is known that if the phases are in nano-size, they do not appear in x- ray diffraction patterns [5], in this way no reflection from γ-Al_2O_3 was observed in the MMC patterns, all of this because, the wt.% of alumina was not enough to enhance XRD peaks intensity, and alumina has a nanometric scale size. The intensity corresponding to the Al_2CuMg phase shows an increase as a function of the alumina concentration until 3.0 wt. %. The reason is because, the alumina has a different thermal expansion coefficient with aluminum matrix, and during sintering and hot extrusion those differences of thermal expansion promote dislocations around the reinforcement phase, and these dislocations are nucleation points for precipitates of: S' (Al_2CuMg) and θ' (Al_2Cu) [14-15]. Above 3.0 wt.% of Al_2O_3 in the MMC, the intensity of these precipitates decreased because the alumina nanoparticles introduce a lot of interfaces, which reduces the whole concentration of vacancies in matrix aluminum and consequently the formation of GPB (Guinier Preston Begaryatsky) zones were suppressed and do not promote the precipitation phases[11, 20].

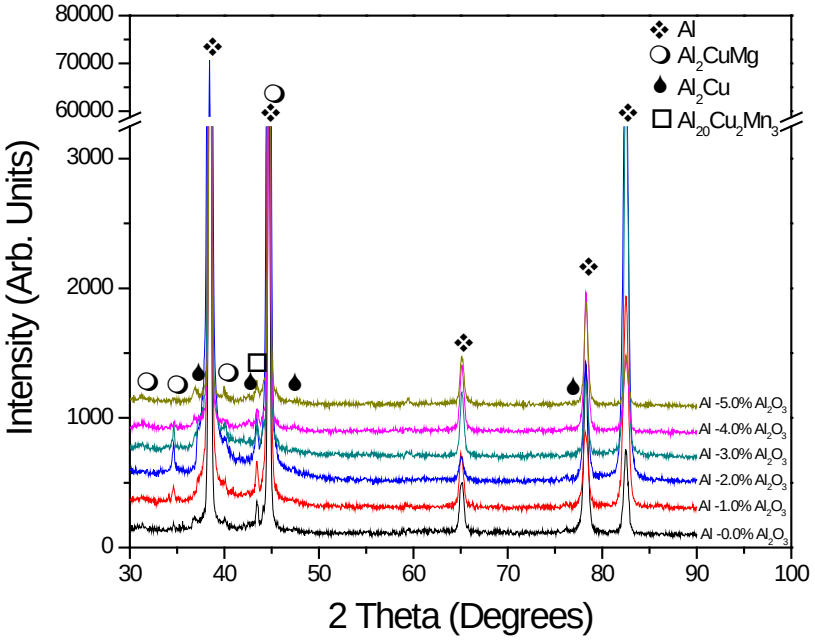

Fig. 3 X ray diffraction Pattern in extruded samples as a function of wt% alumina.

3.3 Microstructural Evolution

Variation on mechanical properties of composites can be explained with microstructural changes in the 2024 aluminum alloy. After mechanical milling, consolidation and hot extrusion processes, samples were analyzed by STEM, TEM and EDS techniques. Some STEM results are shown in Fig. 4. It shows that the nanoparticles of alumina are dispersed and embedded homogeneously into the aluminum matrix material. The result of the EDS analysis of nanoparticles shows the presence of aluminum and oxygen, it is supposed that these nanoparticles (Fig. 4A) correspond to Al_2O_3 dispersoid used to reinforce MMC. Fig. 4B shows the microanalysis in one section of the material, which contains phases of Al-Cu-Mg, according with XRD as shown in Fig. 3 and the reported data [14-15]. We suppose that this phase corresponds to Al_2CuMg. It is known in literature that Al_2CuMg and Al_2Cu can appear as a dispersoid in this kind of aluminum alloy due to the energy input during sintering and the hot extrusion.

The main purpose of applying the mechanical milling process was to generate the homogeneous dispersion of the reinforcement particles. At low concentration (<3.0 wt.%), distribution of reinforcement particles in the aluminum matrix has been successfully obtained, and has also presented effective adhesion with the aluminum matrix, Fig 5. The crystallite size is at nanometric size, generating an increase in the mechanical behavior, as shown in Fig. 1. Note that if nanoparticles are embedded throughout the matrix, these reinforcements should contribute significantly to strengthening mechanisms in the MMC.

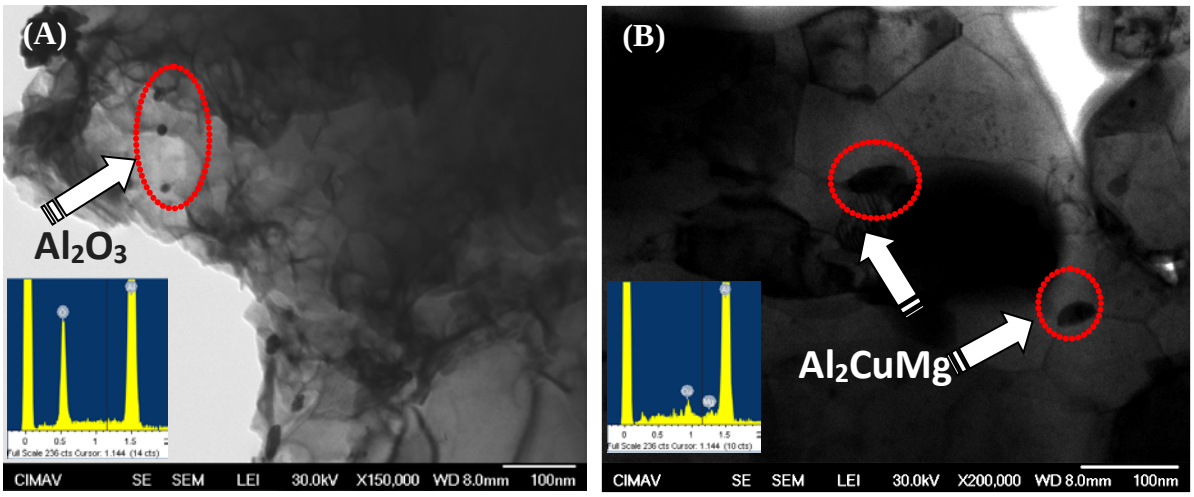

Fig. 4 STEM micrographs and EDS spectrum after milling process and hot extrusion of the Al-2024- 2.0 wt.% Al_2O_3 composite, showing the reinforcement alumina (A), and the presence of precipitate phases (B).

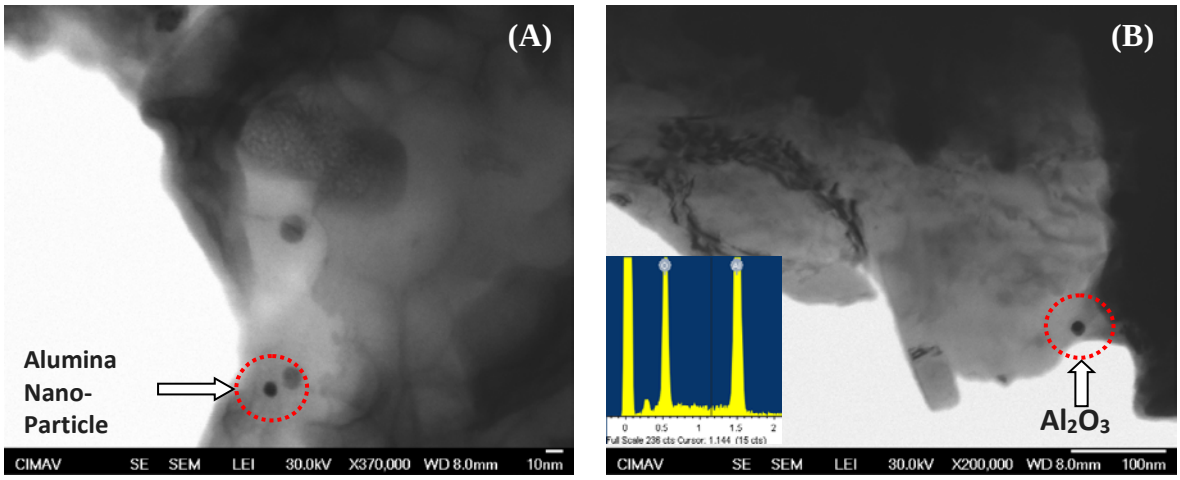

Fig. 5 STEM micrographs and EDS spectrum of the Al-2024- 1.0 wt.% Al_2O_3 specimen. (A and B) Alumina nanoparticle in the structure embedded into the aluminum matrix, and the EDS spectrum of the alumina.

The accelerated grain refinement process by adding nanoparticles could be attributed to the generation of a high dislocation activity, due to interaction between the hard particles and dislocation as H. Chung and Shin have shown it [18]. Because of Al_2O_3 nanoparticles are hard and non-deformable; they can obstruct the dislocation movement, leading to a dislocation density increase. If the ceramic reinforcement particles are in nanoscale size, the Orowan mechanism leads to reproduction of dislocations [11]. Hence, the grain refining process in the nano MMC should be accelerated. This phenomenon is demonstrated in Fig. 5(A), where the substructure has a nano-size crystallite lower than 100nm. It has been reported by Z.Y.Ma and Y. Liang [19], that the strength of the aluminum alloy is related to the particle dislocation interaction according with the Orowan mechanism. Residual dislocation loops are left around; each particle after a dislocation passes the particles.

From Table 2, the composite with 2.0 wt. % alumina nanoparticles shows the best results. The yield and tensile strength were 220.9 MPa and 443.6 MPa respectively; however, at higher nanoparticles concentrations (> 2.0 wt.%) the mechanical properties fall down. It is known that nano-ceramics are very susceptible to agglomeration as Boey Z. Yaun demonstrated on it [16]. The formation of hard agglomerates is expected when nanoscale particles (<100nm) are used. In Fig. 6 (A and B) the MMC, has 4.0 wt. % Al_2O_3, where nano-agglomerations took place in the microstructure, falling the mechanical properties. Agglomerated clusters, confirmed by TEM micrographs and elemental mapping of aluminum and oxygen for the consolidated MMC are shown in Fig. 6 (C, D, E). These agglomerated zones could have a fragile behavior, cracks in agglomerates, interface

breakage, and matrix-particle separation, causing damage in the material matrix. It is known that if the inhomogeneous dispersion appears, the reinforcement reduces the 'effective' amount of particulates for strengthening [11].

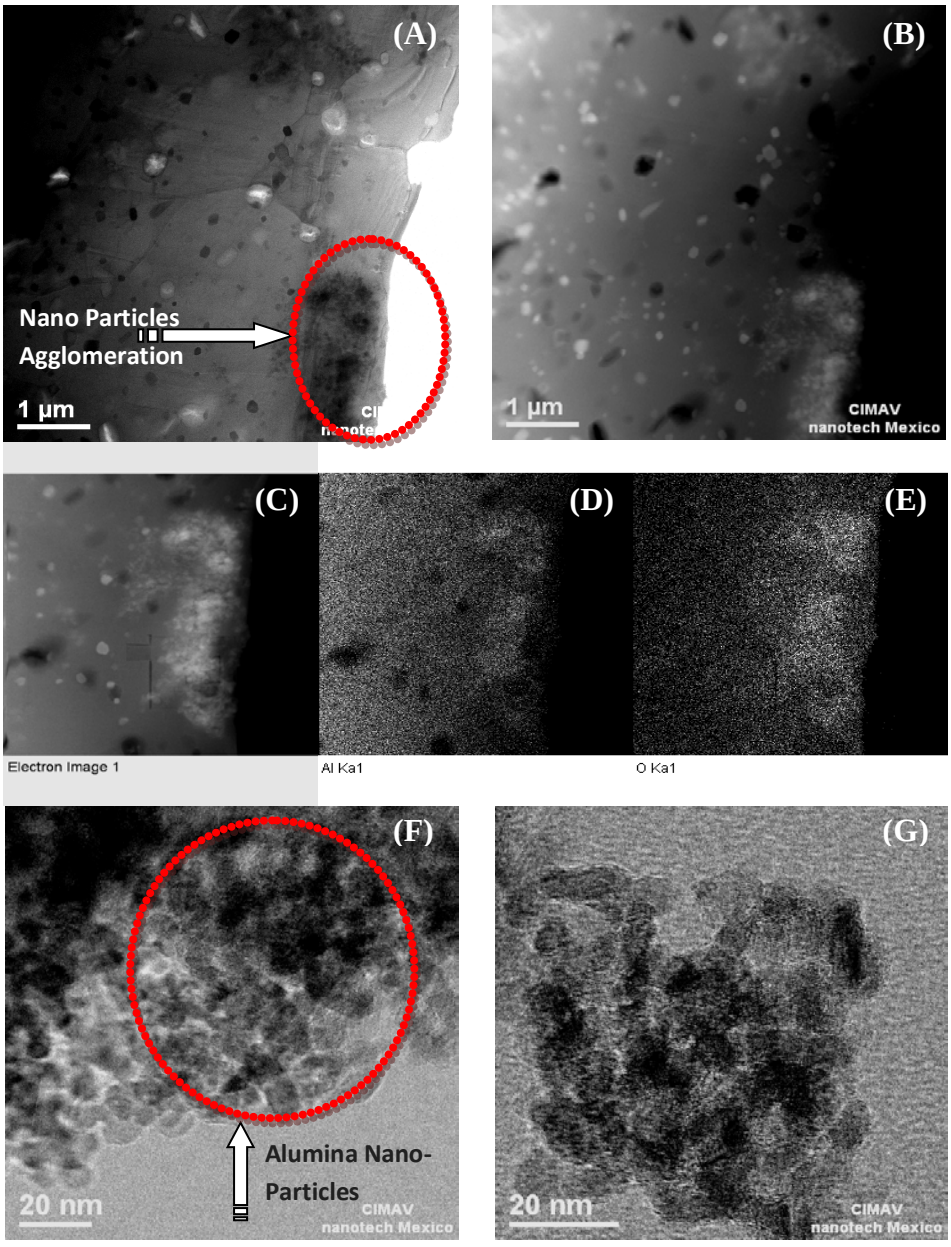

Fig. 6 (A) Bright field, (B) Dark field TEM micrographs of the Al-2024- 4.0 wt.% Al_2O_3 specimen in extrusion condition. Alumina nano-agglomeration particles in the subgrains structure embedded in the aluminum matrix. (C) Electron micrograph in the same zone. (D) and (E) EDS Al-O mapping. (F) and (G) TEM micrographs showing a closer view of alumina nanoparticles in the aluminum composite.

Apparently, neither voids nor cracks can be detected in interface metal-ceramic viewed in Fig. 6 (F and G). Both defects, which could not be easily detected, affect the mechanical properties in composite materials. Agglomeration zones provide sites for crack initiation, from pores in the middle of these zones, generating a bad adhesion with the matrix, and finally the cracks could grow, coalesce and give the fracture of the material.

Another theory for decreasing mechanical properties was provided by Razavi Hesabi et al.[17]. They have reported that the densification rate of milled powder at high pressures is lower than the ones that have not been deformed by mechanical milling. This can be attributed to the hardening effect from mechanical milling, which increased the hardness of the powder particles and consequently limited the plastic deformation of the aluminum alloy. It is important to discuss that the powder density has a strong correlation with the physical morphology and size distribution of the milled particles. Consequently a variation of the shape and the hardness in the powder, change the tendency to make bridges and become densely packed. In samples with 3.0 wt.% of alumina or more reinforcement phase, the flattened morphology of the milling particles are the responsible of lower densifications giving residual porosity in the composite and decreasing of mechanical properties.

The lower tensile properties for the milled composites with higher percentage of reinforcement (> 3.0 wt.% of alumina) could happen as a result of the lower contact area between the aluminum alloy powders, required for suitable plastic deformation during milling, as well as, the elongated shape of the milled powders [21]. This phenomenon creates porosity which is an important factor to reduce mechanical behavior. In this way Naiqin Zhao et al.[4] have examined the increase of hardness in the milled powder, they proposed that the mechanical milling will reduce the compressibility of the MMC powder, generating pores and defects in the microstructure.

When the mass fraction of the nanoparticle in the composite exceeded 2 wt.% of alumina, the mechanical properties were reduced, as shown on Table 2. The effect could be clarified by many factors. Some of them are: when alumina nanoparticles content in the MMC goes over a critical value, the grain would be saturated with nanoparticles, impoverishing the crystallization phases like S', θ' and GPB zones as XRD shown in Fig. 3. Also the hardened powder limited the plastic deformation in aluminum matrix, decreasing the density in the sintering composite and creating porosity, and finally agglomerated zones could have a fragile behavior with interface breakage, and resulting in damage in the aluminum matrix.

The mechanical properties at 2.0 wt.% of alumina nanoparticles were successfully improved, due to several strengthening mechanisms working at the same time; grain refinement produced by MA process, an homogeneous distribution of the reinforcement second phase by the MA, thermal mismatch [22] between Al-2024 and alumina nanoparticles (alumina has a thermal expansion coefficient of 7.5 x 10^{-6} K^{-1}; while 2024-aluminum has a higher one around 24.7 x 10^{-6} K^{-1}) consequently the contraction of the alloy after sintering and the hot extrusion process may contribute to the mechanical adhesion and produce dislocations around the nanoparticles. Also the Orowan looping mechanism, work hardening and the crystallization of the S', T and θ' dispersed in the alloy had contributed to enhance the mechanical behavior in the aluminum composite.

4. Conclusion

Alumina nanoparticles can be introduced to the 2024 aluminum matrix, using mechanical milling process. It demonstrated that the additions of 2.0 wt.% of Al_2O_3 improves the yield and tensile strength up to 200.9 and 443.6 MPa respectively. This amount is considerated as a critical value for the reinforcement ceramic phase. Nevertheless, with 3.0 wt.% or higher values in alumina concentration, the agglomeration takes place, and reduces the effectiveness of the strengthening in the MMC. The most important strengthening mechanisms were: the hardening by dispersion of the second phase, the subsequent effect over the dislocations line movement, grain refinement, thermal mismatch between Al-2024 and alumina nanoparticles creating dislocation, the Orowan mechanism and the precipitation phases like: T, S' and θ'. In this way for higher alumina concentrations; the agglomeration zones, less precipitated phases in the microstructure and lower densification of the aluminum powder causing porosity. All of them decrease the mechanical properties making an important loss of the strength from the composite.

Acknowledgements

The authors sincerely acknowledge for their support to CONACYT and Air Force Office of Science Research, Latin America. Contract No. FA9550/06/1/0524. Thanks to W. Antunez-Florez, C. Carreño-Gallardo, I. Estrada-Guel, K.Campos-Venegas, Torres-Moye, D. Lardizabal-Gutiérrez and R. Torres-Sánchez for their technical assistance.

References

[1] Cintas J, Cuevas F G, Montes J M, Herrera E J, *Scripta Mater* **53** (2005) 1165.

[2] Sameezadeh M, Emamy M, Farhangi H, *Mater Des* **32** (2011) 2157.

[3] Razavi Hesabi Z, Simchi A, Seyed Reihani S M, *Mater Sci Eng A* **428** (2006) 159.

[4] Zhao N, Nash P, Yang X, *J of Mater Proc Tech* **170** (2005) 586.

[5] Hernández J L, Cruz J J, Gomez C, Martínez-Sanchez R, *Mater Trans of Jpn* **6** (2010) 1120.

[6] Jia D C, *Mater Sci Eng A* **289** (2000) 83.

[7] Khakbiz M, Akhlaghi F, *J Alloys Compd* **479** (2009) 334.

[8] Naser J, Riehemann W, Ferkel H, *Mater Sci Eng A* **234** (1997) 467.

[9] Tang F, Hagiwara M, Schoenung J M, *Mater Sci Eng A* **407** (2005) 306.

[10] Ferkel H, Mordike B L, *Mater Sci Eng A* **298** (2001) 193.

[11] Kang Y C, Chan S L, *Mater Chem Phys* **85** (2004) 438.

[12] MatWeb, Online Materials Property Data Sheet, 2012, http://www.matweb.com.

[13] Fagagnolo J B, Robert M H, Torralba J M, *Mater Sci Eng A* **426** (2006) 85.

[14] Cheng S, Zhao Y H, Zhu T, Ma E, *Acta Mater* **55** (2007) 5822.

[15] Wang S C, Starink M J, *Int Mater Rev* **50** (2005) 193.

[16] Boey F Y C, Yuan Z, Khor K A, *Mater Sci Eng A* **252** (1998) 276.

[17] Razavi H Z, Hafizpour H R, Simchi A, *Mater Sci Eng A* **454** (2007) 89.

[18] Chung K H, He J, Shin D H, Schoenung J M, *Mater Sci Eng A* **356** (2003) 23.

[19] Ma Z Y, Li Y L, Liang Y, Zheng F, Bi J, Tjong S C, *Mater Sci Eng A* **219** (1996) 229.

[20] Longtao J, Min Z, Gaohui W, Qiang Z, *Mater Sci Eng A***392** (2005) 366.

[21]Estrada Guel I, Carreño Gallardo C., Mendoza Ruiz D C, Miki Yoshida M, Rocha Rangel E, Martínez Sánchez R, *J Alloys Compd* **483** (2009) 173

[22] Deaquino Lara R, Estrada Guel I, Hinojosa Ruiz G, Flores Campos R, Herrera Ramírez J M, Martínez Sánchez R, *J Alloys Compd* **509** (2011) 5284.